ACS Photonics

pubs.acs.org/journal/apchd5

Article

# Ultralow-Noise K-Band Soliton Microwave Oscillator Using Optical Frequency Division

Rui Niu,[¶] Tian-Peng Hua,[¶] Zhen Shen,[¶] Yu Wang, Shuai Wan, Yu Robert Sun, Weiqiang Wang, Wei Zhao, Guang-Can Guo, Wenfu Zhang,* Wen Liu, Shui-Ming Hu,* and Chun-Hua Dong*

Cite This: *ACS Photonics* 2024, 11, 1412−1418

Read Online

ACCESS | Metrics & More | Article Recommendations | Supporting Information

**ABSTRACT:** Compact, low-noise microwave oscillators are required throughout a wide range of applications such as radar systems, wireless networks, and frequency metrology. Optical frequency division via an optical frequency comb provides a powerful tool for low-noise microwave signal generation. Here, we experimentally demonstrate an optical reference down to 26 GHz frequency division based on the dissipative Kerr soliton comb, which is generated on a CMOS-compatible, high-index doped silica glass platform. The optical reference is generated through two continuous wave lasers locked to an ultralow expansion cavity. The dissipative Kerr soliton comb with a repetition rate of 26 GHz acts as a frequency divider to derive an ultralow-noise microwave oscillator, with a phase noise level of −101.3 dBc/Hz at a 100 Hz offset frequency and −132.4 dBc/Hz at a 10 kHz offset frequency. Furthermore, the Allan deviation of the oscillator reaches $6.4 \times 10^{-13}$ at a 1 s measurement time. Our system is expected to provide an ultralow-noise microwave oscillator for future radar systems and the next generation of wireless networks.

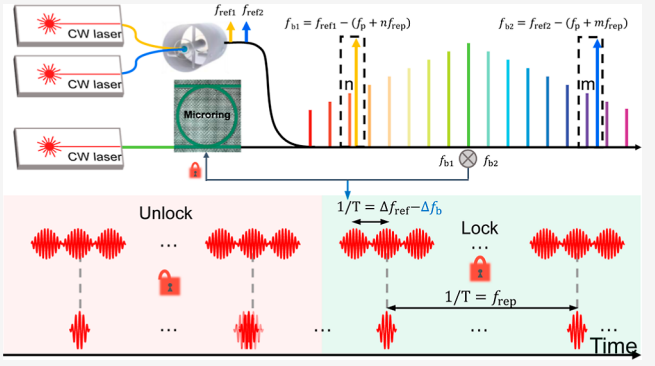


**KEYWORDS:** *microcomb, optical frequency division, microwave oscillator, microcavity, microwave photonics*

## 1. INTRODUCTION

Low-noise microwave signals are crucial for various industrial and scientific applications, including telecommunication networks, radar systems, digital sampling as well as fundamental research in areas such as radio astronomy, laser-driven terahertz electron accelerators, and tests of fundamental constants.[1−6] As the demand for higher-frequency carriers, such as K- and X-bands, grows due to the telecommunications bandwidth bottleneck, generating and digitizing low-noise microwave signals at these frequencies pose increasing challenges. Microwave photonic technologies, which utilize optical devices and techniques to generate, manipulate, and measure high-speed radio frequency (RF) signals, have emerged as a potential solution with superior performance compared to conventional electronics.[7] Thus, the use of photonic to process wideband signals has been widely explored, i.e., dual-mode lasers, Brillouin oscillators, electro-optical dividers, optical delay-line oscillators, and whispering-gallery-mode parametric oscillators.[8−13]

In addition, the optical frequency division (OFD), a method that utilizes optical frequency combs as photonic frequency dividers, shows promise in generating microwaves with excellent frequency stability.[11,14,15] However, most OFD implementations still rely on bulky fiber comb systems with a repetition rate of a few hundred megahertz, making it challenging to synthesize microwave signals beyond the GHz range and introducing complexity due to the need for repetition rate multipliers. Further advancement of these technologies heavily depends on achieving similar performance with photonic integrated components, allowing for miniaturization and improved functionality.

In recent years, the need for integrated dissipative Kerr soliton (DKS) combs makes low-noise, integrated, high frequency band microwave oscillators possible. The DKS naturally produces several GHz-THz comb spectra via four-wave mixing in the optical resonator.[16−28] Also, integrated DKSs have seen rapid development thanks to microfabrication advancements.[29,30] To reduce the phase noise of the DKS oscillator, the OFD principle has been introduced,[31] in which the stability of the oscillator is derived from a stabilized laser. Meanwhile, it is essential to detect and remove the carrier envelope offset frequency ($f_{ceo}$), thus the octave-spanning comb spectra are indispensable in the work. One method of

Received: September 1, 2023
Revised: February 28, 2024
Accepted: February 28, 2024
Published: March 14, 2024

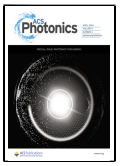







https://doi.org/10.1021/acsphotonics.3c01247
*ACS Photonics* 2024, 11, 1412−1418

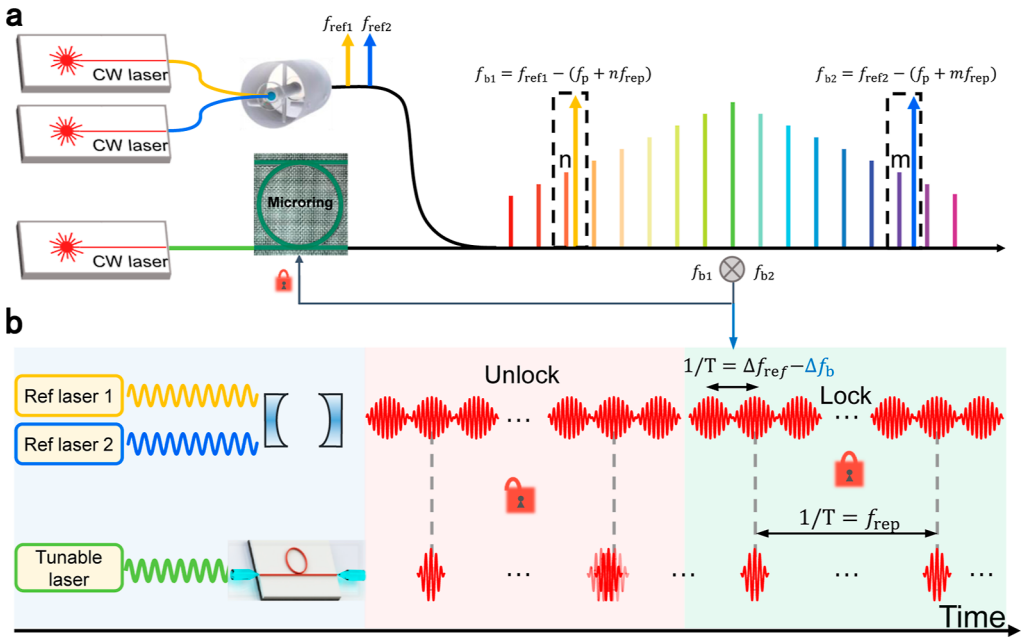


**Figure 1.** (a) Schematic of the optical-to-microwave division circuit. Two reference lasers are locked to one reference cavity. Also, the locked reference lasers are combined with the DKS comb to transfer the relative stability of lasers to the repetition rate of the DKS comb. (b) Time interval between soliton pulses is synchronized with the optical reference through active feedback. *T*: time period.

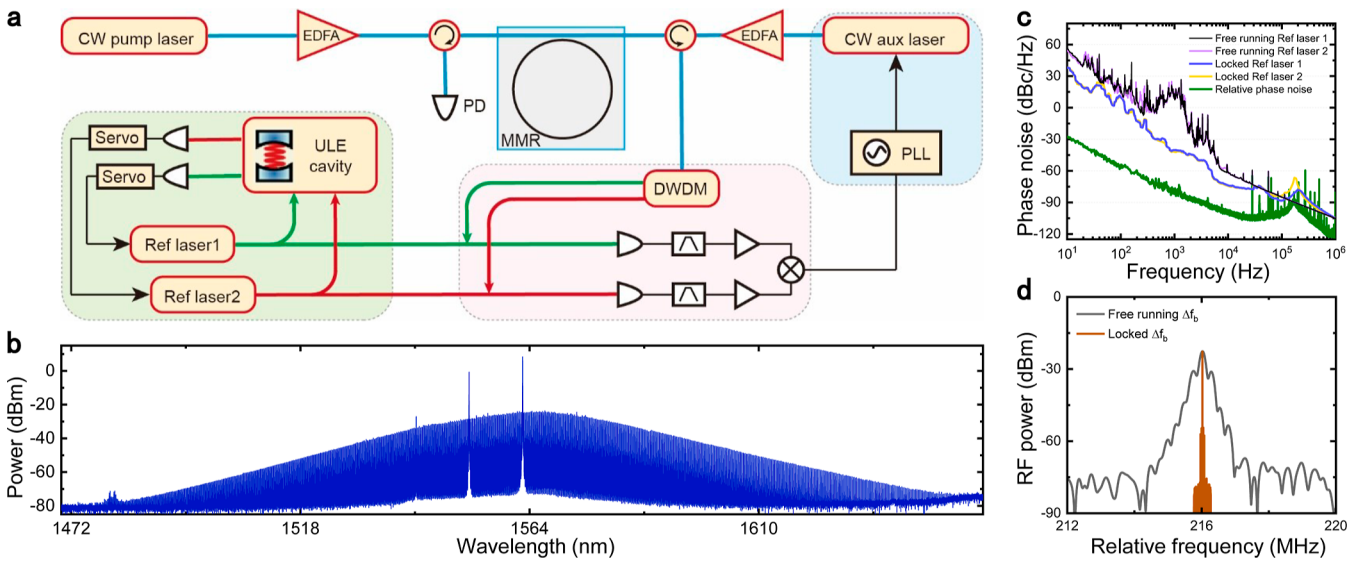


**Figure 2.** (a) Schematic of the experimental setup. An auxiliary laser-assisted thermal balance scheme is employed for DKS generation. The reference lasers are locked to the ULE cavity through PDH locking. The locked reference lasers are combined with the DKS to generate the beat signal. The beat signals are filtered, amplified, and mixed to generate the error signal. The error signal is fed back to the auxiliary laser through the PLL loop. EDFA: erbium-doped fiber amplifier; PD: photodetector; ULE cavity: ultralow expansion cavity; DWDM: dense wavelength division multiplexing; MRR: microring resonator; and PLL: phase lock loop. (b) Optical spectrum of the DKS comb. (c) Measured phase noise of the unlocked (black and purple) and locked reference (blue and yellow) lasers. The corresponding relative phase noise of the locked reference laser is also shown with a green curve. (d) RF spectrum of the mixed beat signal before (gray) and after (brown) locking.

eliminating the need for $f_{ceo}$ involves introducing a pair of stabilized lasers.[32−35] Although promising, this technique needs further refinement to improve its current phase noise level, particularly at near carrier frequencies such as 100 Hz. This frequency offset holds significant importance for slow targets in radar applications.

In this paper, we present the demonstration of an ultralow-noise K-band soliton microwave oscillator, utilizing a micro-comb-based optical-to-microwave frequency division. The DKS is generated on a CMOS-compatible platform, and two comb lines are locked to the stabilized lasers, which are referenced to an ultralow expansion (ULE) cavity. As a result, the phase noise of the oscillator is dependent on the relative phase noise of the stabilized lasers, effectively canceling the free-running pump laser frequency noise or carrier frequency noise. By implementing this method, the phase noise performance of the generated 26 GHz microwave oscillator achieves −101.3 dBc/Hz at a 100 Hz offset frequency and −132.4 dBc/Hz at a 10 kHz offset frequency. Moreover, the oscillator's stability shows improvement as evidenced by an


https://doi.org/10.1021/acsphotonics.3c01247
ACS Photonics 2024, 11, 1412−1418

Allan deviation of 6.4 × $10^{-13}$ at 1 s measurement time. Overall, our work provides a potential pathway toward ultralow-noise microwave oscillators, which holds promise for a range of applications, including radar systems and the next generation of wireless networks.

## 2. SCHEMATIC

The schematic of the ultralow-noise soliton microwave oscillator is illustrated in Figure 1a. Two individual lasers are locked to one reference cavity, and the relative phase noise of these two lasers could be reduced.[11] Then, these two lasers are beating with the DKS generated in a microring, and the beating signals are generated at RF values of

$$f_{b1} = f_{ref1} - (n \times f_{rep} + f_p) \quad (1)$$

$$f_{b2} = f_{ref2} - (m \times f_{rep} + f_p) \quad (2)$$

where $f_{ref1}$ and $f_{ref2}$ are the frequencies of reference lasers. $f_{rep}$ and $f_p$ are the repetition rate frequency and the frequency of the pump laser, respectively. $n$ and $m$ are the relative mode numbers of comb lines nearest to the reference lasers with respect to the pump resonance mode. The difference $(f_{b1} - f_{b2}) - (f_{ref1} - f_{ref2}) = (m - n)f_{rep}$ is an integral multiple of the repetition rate. By taking the difference of $f_{b1}$ and $f_{b2}$, the phase fluctuation of $f_p$ is removed.[32] The phase fluctuation of $\triangle f_b = f_{b1} - f_{b2}$ could be minimized through referencing to the external frequency reference, i.e., a rubidium clock. Also, the phase fluctuation of $f_{rep}$ is dominated by the relative phase noise of reference lasers and the relative mode number of comb lines. Considering the residual phase error ($\delta\varepsilon$) due to the phase lock loop (PLL), the phase noise of the repetition rate could be expressed as

$$\langle \delta^2_{f_{rep}} \rangle = \frac{\langle \delta^2_{f_{ref1} - f_{ref2}} \rangle + \langle \delta\varepsilon^2 \rangle}{(n - m)^2} \quad (3)$$

Since the residual phase error due to the PLL could be ignored, the phase noise of $f_{rep}$ is reduced from the relative phase noise of the reference lasers by the square of the relative mode number of comb lines. From a temporal viewpoint as shown in Figure 1b, the two light beams locked to the ULE cavity produce beat frequency at the THz level, serving as an optical reference. The time interval of soliton pulses is synchronized with the optical reference using active feedback, leading to an enhancement in the phase noise of the repetition frequency. Furthermore, considering the unit of phase noise of $f_{rep}$, the reduction factor could be expressed as $20 \times \log\frac{f_{ref1} - f_{ref2}}{f_{rep}}$. In our work, the DKS is generated in a microring resonator (MRR), which is fabricated on a CMOS-compatible, high-index doped silica glass platform and packaged into a 14-pin butterfly package with a thermo-electric cooler chip.[36,37] The $Q$-factor and free spectral range of the MRR are about 2.2 × $10^6$ and 26 GHz, respectively. A tunable laser (Toptica CTL 1550) is amplified to generate the soliton microcomb while another auxiliary laser is also amplified and coupled into the MRR in the opposite direction to balance the thermal effect in the microcavity.[38−42] Two circulators are used to prevent the residual light from being injected into the erbium-doped fiber amplifier (EDFA) as shown in Figure 2a. With the sufficiency pump power, the DKS comb is generated from 182 to 203 THz, corresponding to a frequency range of 21 THz as shown in Figure 2b. Thus, the maximum reduction factor could be estimated as $20 \times \log\frac{21\ \text{THz}}{26\ \text{GHz}} = 58.1$ dB in our work.

## 3. RESULTS

To achieve the ultralow-noise K-band soliton microwave oscillator, the DKS is directly sent to a DWDM system, which spectrally selects two comb lines of interest to beat with the reference lasers at photodiodes (PD). The reference lasers are locked to an ULE cavity with a finesse of 150,000 and a free spectral range of 1.5 GHz. The single sideband phase noise of the reference lasers is evaluated using a self-heterodyne interferometer[43] as depicted by the yellow and blue lines in Figure 2c. The phase noise of both reference lasers is recorded at levels of −39.8 dBc/Hz at a 1 kHz offset and −73.8 dBc/Hz at a 10 kHz offset, exhibiting a clear improvement over the free-running laser as indicated by the black and purple lines in Figure 2c. Additionally, we have measured the relative phase noise of the reference lasers with a two-wavelength delayed self-heterodyne interferometer,[44,45] which is an imbalanced Mach−Zehnder interferometer that incorporates an acousto-

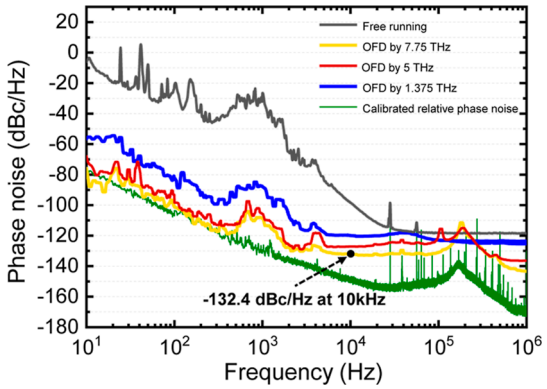


**Figure 3.** Phase noise of the 26 GHz signal with various span of reference lasers and the green curve shows the calibrated relative phase noise of the reference lasers.

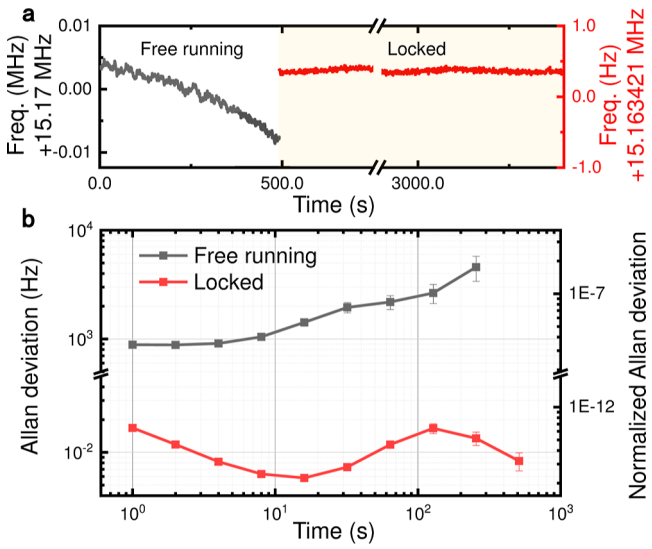


**Figure 4.** (a) Time trace of the **26 GHz** signal. (b) Allan deviation of the **26 GHz** signal in free-running operation (black curve) and locked to the optical reference (red curve). Error bars represent a 68% confidence interval.


https://doi.org/10.1021/acsphotonics.3c01247
ACS Photonics 2024, 11, 1412−1418

Table 1. Comparison with Other Reported Soliton Microwave Oscillators

| material | configuration | carrier freq. (GHz) | phase noise at 100 Hz (dBc/Hz, scaled to 26 GHz) | phase noise at 10 kHz (dBc/Hz, scaled to 26 GHz) | relative Allan deviation@1 s |
|---|---|---|---|---|---|
| $Si_3N_4$[46] | free run | 19.6 | −42.5 | −107.5 | $8 \times 10^{-8}$ |
| $SiO_2$[47] | quiet point | 11 | −72.5 | −125.5 | |
| $SiO_2$[48] | quiet point | 15 | −63.2 | −108.2 | $2 \times 10^{-10}$ |
| $MgF_2$[49] | injection locking | 14 | −71.6 | −123.6 | $2 \times 10^{-12}$ |
| $MgF_2$[50] | self-injection locked pump | 9.9 | −81.6 | −116.6 | $1 \times 10^{-11}$ |
| $MgF_2$[31] | USL pump + OFD + $f_{ceo}$ detection | 14 | −79.6 | −129.6 | |
| $MgF_2$[33] | OFD | 10.3 | −82.0 | −107.0 | |
| $Si_3N_4$[32] | OFD | 300 | −55.2 | −129.2 | |
| $SiO_2$[35] | OFD | 22 | −86.6 | −123.6 | $9 \times 10^{-13}$ |
| doped $SiO_2$ (this work) | OFD | 26 | −101.3 | −132.4 | $6 \times 10^{-13}$ |

optic modulator in the short arm. By measuring the phase noise power spectrum density of the mixed photodetected signal, we can determine the relative phase noise of the reference lasers.[44,45] The green line in Figure 2c depicts the relative phase noise of the two reference lasers separated by 7.75 THz. Furthermore, the relative phase noise of the reference lasers shows a notable reduction from 10 Hz to 10 kHz, and at higher offset frequencies, it is governed by the servo loop.

When the relative phase noise of two reference lasers is down-converted to 26 GHz in the OFD experiment, the phase noise of the microwave is suppressed by a reduction factor. To achieve that, the generated beat signals are amplified, filtered, and mixed to generate an intermediate RF signal (represented by the gray curve in Figure 2d). The $f_p$ noise is canceled out according to eq 3. The repetition rate could be tuned by the auxiliary laser frequency without changing the pump laser frequency based on the thermo-optic effect.[42] Therefore, the intermediate RF signal is subsequently converted to direct current and fed back to the current modulation input of the auxiliary laser through a PLL. When the intermediate RF signal is locked to the external frequency reference, the phase noise of the two reference lasers is down-converted to 26 GHz. By analyzing the RF signal in Figure 2d, we can observe the effectiveness of the phase-locked loop, as it exhibits a coherent peak indicative of a locked operation, in contrast to free-running operation. The ultimate line width of the intermediate RF signal is determined by the PLL and the external frequency reference, which in our case is a rubidium clock. Additionally, the phase noise of the repetition rate is detected using a fast photodetector (Newport 1014) and measured with a phase noise analyzer (Rohde & Schwarz FSWP). Similarly, the phase noise demonstrates a noticeable reduction after the locking operation.

The phase noise measurements of the soliton microwave oscillator are presented in Figure 3. With OFD, the phase noise of the $f_{rep}$ exhibits a significant reduction compared to that of the free-running state. The phase noise reaches −118.2 dBc/Hz at a 10 kHz offset frequency with a 1.375 THz optical span. To further optimize the phase noise, we adjust the optical span of the reference lasers by locking them to the same mode family at different wavelengths. The phase noise of the generated ultralow-noise 26 GHz signal with various optical span is shown in Figure 3. For different optical span (1.375 and 7.75 THz), the reduction factors can be calculated with $20 \times \log\frac{1.375\ \text{THz}}{26\ \text{GHz}} = 34.5\ \text{dB}$ and $20 \times \log\frac{7.75\ \text{THz}}{26\ \text{GHz}} = 49.5\ \text{dB}$, thus corresponding phase noise are, respectively, −118.2, and −132.4 dBc/Hz at a 10 kHz offset frequency. Also, the relative phase noise of the 7.75 THz frequency separation with a reduction factor 49.5 dB is shown as the calibrated phase noise. As depicted in Figure 3, the calibrated relative phase noise and the measured phase noise of $f_{rep}$ divided by the optical span of 7.75 THz agree well within the 10 Hz to several kHz offset frequency range. At higher offset frequencies, the phase noise of the oscillator is limited by the bandwidth of the PLL, resulting in a mismatch with the calibrated relative phase noise due to PLL servo locking bumps. To further optimize the phase noise, the optical span of the reference lasers can be increased. Considering the span and repetition rate of our DKS comb, the maximum reduction factor could reach 58.1 dB, which was limited by the bandwidth of the commercial DWDM used in our experiment. Additionally, with the effective filter element, the ultimate phase noise could reach approximately −141 dBc/Hz at a 10 kHz offset frequency using our OFD system.

In order to fully characterize the oscillator, it is crucial to evaluate its mid- and long-term stability. We recorded the frequency variation of the repetition rate using a frequency counter with a gate time of 1 s. Due to the detection range limitations of our frequency counter, the repetition rate is down-converted to a frequency below 300 MHz using an electro-optic modulator.[41] The frequency counter is referenced to a 10 MHz output from a rubidium clock. Figure 4a displays the down-converted frequency over a period of 1000 s, distinguishing between the free-running operation of the DKS and when it is locked to the optical reference. The 26 GHz signal demonstrates increased stability when in locked operation. Furthermore, we express the fractional instability of the 26 GHz signal in terms of the Allan deviation as shown in Figure 4b. The free-running state of the DKS exhibits a stability of $3.4 \times 10^{-8}$ at a 1 s measurement time. Locking the DKS to the optical reference improved the stability level to $6.4 \times 10^{-13}$.

## 4. CONCLUSION

In conclusion, we demonstrate an ultralow-noise soliton microwave oscillator using OFD. The system is built upon the CMOS-compatible, high-index doped silica glass platform. The optical reference lasers are locked to the ULE cavity to minimize the relative phase noise. Also, the comb lines of the DKS comb are referenced to the optical reference to reduce the phase noise of the repetition. The soliton microwave



https://doi.org/10.1021/acsphotonics.3c01247
ACS Photonics 2024, 11, 1412−1418

oscillator generates a stable 26 GHz signal with a phase noise of −101.3 dBc/Hz at a 100 Hz offset frequency and −132.4 dBc/Hz at a 10 kHz offset frequency. Table 1 provides a comprehensive comparison of the soliton microwave oscillators. It is evident that we achieve the most optimal phase noise at a 100 Hz offset frequency (scaled to 26 GHz). Additionally, our phase noise performance is comparable to the OFD scheme based on $f_{ceo}$ detection at a 10 kHz offset frequency and outperforms the dual-reference-based OFD scheme (used in our work). Notably, this scheme relaxes the requirement for octave-spanning combs.

Currently, the ultimate phase noise of our oscillator is limited by the bandwidth of the DWDM, which could be replaced by a custom Bragg grating or microcavity filter. With the effective filter element, the ultimate phase noise could reach about −141 dBc/Hz at a 10 kHz offset frequency according to the optical span and the repetition rate of our DKS comb. In addition, the auxiliary-laser-assisted soliton generation method can be refined by utilizing the frequency-scanning technique[51] and the thermal tuning approach,[52] and the EDFA can be integrated onto the chip.[53] With increasing the $Q$ factor of the microring, the external EDFA may be eliminated altogether.[52] Moreover, the ULE cavity in our system could be replaced with recently demonstrated integrated devices,[54] which provides a promising option for compact ultralow-noise microwave oscillator generation.

## ■ ASSOCIATED CONTENT

### Data Availability Statement

The data that support the plots within this paper and other findings of this study are available from the corresponding author on reasonable request.

### Supporting Information

The Supporting Information is available free of charge at https://pubs.acs.org/doi/10.1021/acsphotonics.3c01247.

Technical details on the experimental setup, measurements of the phase noise, and additional data on the phase noise of the 26 GHz signal (PDF)

## ■ AUTHOR INFORMATION


### Corresponding Authors

**Wenfu Zhang** − *State Key Laboratory of Transient Optics and Photonics, Xi'an Institute of Optics and Precision Mechanics, CAS, Xi'an 710119, China; University of Chinese Academy of Sciences, Beijing 100049, China*; Email: wfuzhang@opt.ac.cn

**Shui-Ming Hu** − *CAS Center for Excellence in Quantum Information and Quantum Physics, University of Science and Technology of China, Hefei 230088, China; Department of Chemical Physics, University of Science and Technology of China, Hefei 230026, China; Hefei National Laboratory, University of Science and Technology of China, Hefei, Anhui 230088, China*; orcid.org/0000-0002-1565-8468; Email: smhu@ustc.edu.cn

**Chun-Hua Dong** − *CAS Key Laboratory of Quantum Information, University of Science and Technology of China, Hefei 230026, China; CAS Center for Excellence in Quantum Information and Quantum Physics, University of Science and Technology of China, Hefei 230088, China; Hefei National Laboratory, University of Science and Technology of China, Hefei, Anhui 230088, China*; orcid.org/0000-0002-9408-6102; Email: chunhua@ustc.edu.cn

### Authors

**Rui Niu** − *CAS Key Laboratory of Quantum Information, University of Science and Technology of China, Hefei 230026, China; CAS Center for Excellence in Quantum Information and Quantum Physics, University of Science and Technology of China, Hefei 230088, China; Hefei National Laboratory, University of Science and Technology of China, Hefei, Anhui 230088, China*

**Tian-Peng Hua** − *CAS Center for Excellence in Quantum Information and Quantum Physics, University of Science and Technology of China, Hefei 230088, China; Department of Chemical Physics, University of Science and Technology of China, Hefei 230026, China*

**Zhen Shen** − *CAS Key Laboratory of Quantum Information, University of Science and Technology of China, Hefei 230026, China; CAS Center for Excellence in Quantum Information and Quantum Physics, University of Science and Technology of China, Hefei 230088, China; Hefei National Laboratory, University of Science and Technology of China, Hefei, Anhui 230088, China*

**Yu Wang** − *CAS Key Laboratory of Quantum Information, University of Science and Technology of China, Hefei 230026, China; CAS Center for Excellence in Quantum Information and Quantum Physics, University of Science and Technology of China, Hefei 230088, China; Hefei National Laboratory, University of Science and Technology of China, Hefei, Anhui 230088, China*

**Shuai Wan** − *CAS Key Laboratory of Quantum Information, University of Science and Technology of China, Hefei 230026, China; CAS Center for Excellence in Quantum Information and Quantum Physics, University of Science and Technology of China, Hefei 230088, China; Hefei National Laboratory, University of Science and Technology of China, Hefei, Anhui 230088, China*

**Yu Robert Sun** − *CAS Center for Excellence in Quantum Information and Quantum Physics, University of Science and Technology of China, Hefei 230088, China; Department of Chemical Physics, University of Science and Technology of China, Hefei 230026, China*

**Weiqiang Wang** − *State Key Laboratory of Transient Optics and Photonics, Xi'an Institute of Optics and Precision Mechanics, CAS, Xi'an 710119, China; University of Chinese Academy of Sciences, Beijing 100049, China*; orcid.org/0000-0002-1157-0370

**Wei Zhao** − *State Key Laboratory of Transient Optics and Photonics, Xi'an Institute of Optics and Precision Mechanics, CAS, Xi'an 710119, China; University of Chinese Academy of Sciences, Beijing 100049, China*

**Guang-Can Guo** − *CAS Key Laboratory of Quantum Information, University of Science and Technology of China, Hefei 230026, China; CAS Center for Excellence in Quantum Information and Quantum Physics, University of Science and Technology of China, Hefei 230088, China; Hefei National Laboratory, University of Science and Technology of China, Hefei, Anhui 230088, China*

**Wen Liu** − *Department of Optics and Optical Engineering, University of Science and Technology of China, Hefei 230026, China*

Complete contact information is available at: https://pubs.acs.org/10.1021/acsphotonics.3c01247

### Author Contributions

[¶]R.N., T.-P.H., and Z.S. contributed equally to this work.

### Funding

The work was supported by the National Key R&D Program of China (grant no. 2020YFB2205801), Innovation program for Quantum Science and Technology (2021ZD0303203 and 2021ZD0303102), the National Natural Science Foundation of China (12293050, 12293052, 11934012, 12104442, 92050109, 92250302, and 12304435), the CAS Project for Young Scientists in Basic Research (YSBR-069), the Fundamental Research Funds for the Central Universities, the China Postdoctoral Science Foundation (2023M733414), Anhui Provincial Natural Science Foundation (grant no. 2308085J12), and the Postdoctoral Fellowship Program of CPSF (GZC20232564).

### Notes

The authors declare no competing financial interest.

## ■ ACKNOWLEDGMENTS

The authors thank R. Zhao and B. Yang for assistance. This work was partially carried out at the USTC Center for Micro and Nanoscale Research and Fabrication.

## ■ REFERENCES

(1) Koenig, S.; Lopez-Diaz, D.; Antes, J.; Boes, F.; Henneberger, R.; Leuther, A.; Tessmann, A.; Schmogrow, R.; Hillerkuss, D.; Palmer, R.; et al. Wireless sub-THz communication system with high data rate. *Nat. Photonics* **2013**, *7*, 977−981.

(2) Maleki, L. The optoelectronic oscillator. *Nat. Photonics* **2011**, *5*, 728−730.

(3) Valley, G. C. Photonic analog-to-digital converters. *Opt. Express* **2007**, *15*, 1955−1982.

(4) Brünken, S.; Sipilä, O.; Chambers, E. T.; Harju, J.; Caselli, P.; Asvany, O.; Honingh, C. E.; Kamiński, T.; Menten, K. M.; Stutzki, J.; Schlemmer, S. $H_2D^+$ observations give an age of at least one million years for a cloud core forming Sun-like stars. *Nature* **2014**, *516*, 219−221.

(5) Zhang, D.; Fallahi, A.; Hemmer, M.; Wu, X.; Fakhari, M.; Hua, Y.; Cankaya, H.; Calendron, A.-L.; Zapata, L. E.; Matlis, N. H.; Kärtner, F. X. Segmented terahertz electron accelerator and manipulator (STEAM). *Nat. Photonics* **2018**, *12*, 336−342.

(6) Nagel, M.; Parker, S. R.; Kovalchuk, E. V.; Stanwix, P. L.; Hartnett, J. G.; Ivanov, E. N.; Peters, A.; Tobar, M. E. Direct terrestrial test of Lorentz symmetry in electrodynamics to $10^{-18}$. *Nat. Commun.* **2015**, *6*, 8174.

(7) Marpaung, D.; Yao, J.; Capmany, J. Integrated microwave photonics. *Nat. Photonics* **2019**, *13*, 80−90.

(8) Callahan, P. T.; Gross, M. C.; Dennis, M. L. Phase noise measurements of a dual-wavelength Brillouin fiber laser. In *2010 IEEE International Topical Meeting on Microwave Photonics*, 2010; pp 155−158.

(9) Li, J.; Lee, H.; Vahala, K. J. Microwave synthesizer using an on-chip Brillouin oscillator. *Nat. Commun.* **2013**, *4*, 2097.

(10) Bai, Y.; Zhang, M.; Shi, Q.; Ding, S.; Qin, Y.; Xie, Z.; Jiang, X.; Xiao, M. Brillouin-Kerr soliton frequency combs in an optical microresonator. *Phys. Rev. Lett.* **2021**, *126*, 063901.

(11) Li, J.; Yi, X.; Lee, H.; Diddams, S. A.; Vahala, K. J. Electro-optical frequency division and stable microwave synthesis. *Science* **2014**, *345*, 309−313.

(12) Eliyahu, D.; Seidel, D.; Maleki, L. Phase noise of a high performance OEO and an ultra low noise floor cross-correlation microwave photonic homodyne system. In *2008 IEEE International Frequency Control Symposium*, 2008; pp 811−814.

(13) Savchenkov, A. A.; Rubiola, E.; Matsko, A. B.; Ilchenko, V. S.; Maleki, L. Phase noise of whispering gallery photonic hyperparametric microwave oscillators. *Opt. Express* **2008**, *16*, 4130−4144.

(14) Fortier, T. M.; Kirchner, M. S.; Quinlan, F.; Taylor, J.; Bergquist, J.; Rosenband, T.; Lemke, N.; Ludlow, A.; Jiang, Y.; Oates, C.; Diddams, S. A. Generation of ultrastable microwaves via optical frequency division. *Nat. Photonics* **2011**, *5*, 425−429.

(15) Li, J.; Vahala, K. Small-sized, ultra-low phase noise photonic microwave oscillators at X-Ka bands. *Optica* **2023**, *10*, 33−34.

(16) Suh, M.-G.; Vahala, K. Gigahertz-repetition-rate soliton microcombs. *Optica* **2018**, *5*, 65−66.

(17) Tan, T.; Yuan, Z.; Zhang, H.; Yan, G.; Zhou, S.; An, N.; Peng, B.; Soavi, G.; Rao, Y.; Yao, B. Multispecies and individual gas molecule detection using Stokes solitons in a graphene over-modal microresonator. *Nat. Commun.* **2021**, *12*, 6716.

(18) Shu, H.; Chang, L.; Tao, Y.; Shen, B.; Xie, W.; Jin, M.; Netherton, A.; Tao, Z.; Zhang, X.; Chen, R.; Bai, B.; Qin, J.; Yu, S.; Wang, X.; Bowers, J. E. Microcomb-driven silicon photonic systems. *Nature* **2022**, *605*, 457−463.

(19) Chen, H.-J.; Ji, Q.-X.; Wang, H.; Yang, Q.-F.; Cao, Q.-T.; Gong, Q.; Yi, X.; Xiao, Y.-F. Chaos-assisted two-octave-spanning microcombs. *Nat. Commun.* **2020**, *11*, 2336.

(20) Zhang, S.; Silver, J. M.; Shang, X.; Del Bino, L.; Ridler, N. M.; DelHaye, P. Terahertz wave generation using a soliton microcomb. *Opt. Express* **2019**, *27*, 35257−35266.

(21) Liu, J.; Bo, F.; Chang, L.; Dong, C.-H.; Ou, X.; Regan, B.; Shen, X.; Song, Q.; Yao, B.; Zhang, W.; Zou, C.; Xiao, Y. Emerging material platforms for integrated microcavity photonics. *Sci. China: Phys., Mech. Astron.* **2022**, *65*, 104201.

(22) Wan, S.; Niu, R.; Wang, Z.-Y.; Peng, J.-L.; Li, M.; Li, J.; Guo, G.-C.; Zou, C.-L.; Dong, C.-H. Frequency stabilization and tuning of breathing solitons in $Si_3N_4$ microresonators. *Photonics Res.* **2020**, *8*, 1342−1349.

(23) Wang, W.; Wang, L.; Zhang, W. Advances in soliton microcomb generation. *Adv. Photonics* **2020**, *2*, 034001.

(24) Sun, Z.; Li, Y.; Bai, B.; Zhu, Z.; Sun, H. Silicon nitride-based Kerr frequency combs and applications in metrology. *Adv. Photonics* **2022**, *4*, 064001.

(25) Xue, X.; Wang, P.-H.; Xuan, Y.; Qi, M.; Weiner, A. M. Microresonator Kerr frequency combs with high conversion efficiency. *Laser Photonics Rev.* **2017**, *11*, 1600276.

(26) Obrzud, E.; Rainer, M.; Harutyunyan, A.; Anderson, M. H.; Liu, J.; Geiselmann, M.; Chazelas, B.; Kundermann, S.; Lecomte, S.; Cecconi, M.; et al. A microphotonic astrocomb. *Nat. Photonics* **2019**, *13*, 31−35.

(27) Wang, C.; Li, J.; Yi, A.; Fang, Z.; Zhou, L.; Wang, Z.; Niu, R.; Chen, Y.; Zhang, J.; Cheng, Y.; et al. Soliton formation and spectral translation into visible on CMOS-compatible 4H-silicon-carbide-on-insulator platform. *Light: Sci. Appl.* **2022**, *11*, 341.

(28) Wang, B.; Morgan, J. S.; Sun, K.; Jahanbozorgi, M.; Yang, Z.; Woodson, M.; Estrella, S.; Beling, A.; Yi, X. Towards high-power, high-coherence, integrated photonic mmWave platform with microcavity solitons. *Light: Sci. Appl.* **2021**, *10*, 4.

(29) Shen, B.; Chang, L.; Liu, J.; Wang, H.; Yang, Q. F.; Xiang, C.; Wang, R. N.; He, J.; Liu, T.; Xie, W.; et al. Integrated turnkey soliton microcombs. *Nature* **2020**, *582*, 365−369.

(30) Xiang, C.; Liu, J.; Guo, J.; Chang, L.; Wang, R. N.; Weng, W.; Peters, J.; Xie, W.; Zhang, Z.; Riemensberger, J.; Selvidge, J.; Kippenberg, T. J.; Bowers, J. E. Laser soliton microcombs heterogeneously integrated on silicon. *Science* **2021**, *373*, 99−103.

(31) Lucas, E.; Brochard, P.; Bouchand, R.; Schilt, S.; Südmeyer, T.; Kippenberg, T. J. Ultralow-noise photonic microwave synthesis using a soliton microcomb-based transfer oscillator. *Nat. Commun.* **2020**, *11*, 374.

(32) Tetsumoto, T.; Nagatsuma, T.; Fermann, M. E.; Navickaite, G.; Geiselmann, M.; Rolland, A. Optically referenced 300 GHz millimetre-wave oscillator. *Nat. Photonics* **2021**, *15*, 516−522.

(33) Weng, W.; Anderson, M. H.; Siddharth, A.; He, J.; Raja, A. S.; Kippenberg, T. J. Coherent terahertz-to-microwave link using electro-optic-modulated turing rolls. *Phys. Rev. A* **2021**, *104*, 023511.

(34) Kudelin, I.; Groman, W.; Ji, Q.-X.; Guo, J.; Kelleher, M. L.; Lee, D.; Nakamura, T.; McLemore, C. A.; Shirmohammadi, P.; Hanifi, S.;

et al. Photonic chip-based low noise microwave oscillator. *arXiv* **2023**, arXiv:2307.08937.
(35) Kwon, D.; Jeong, D.; Jeon, I.; Lee, H.; Kim, J. Ultrastable microwave and soliton-pulse generation from fibre-photonic-stabilized microcombs. *Nat. Commun.* **2022**, *13*, 381.
(36) Wang, X.; Xie, P.; Wang, W.; Wang, Y.; Lu, Z.; Wang, L.; Chu, S. T.; Little, B. E.; Zhao, W.; Zhang, W. Program-controlled single soliton microcomb source. *Photonics Res.* **2021**, *9*, 66−72.
(37) Lu, Z.; Chen, H.-J.; Wang, W.; Yao, L.; Wang, Y.; Yu, Y.; Little, B.; Chu, S.; Gong, Q.; Zhao, W.; Yi, X.; Xiao, Y.-F.; Zhang, W. Synthesized soliton crystals. *Nat. Commun.* **2021**, *12*, 3179.
(38) Wang, W.; Lu, Z.; Zhang, W.; Chu, S. T.; Little, B. E.; Wang, L.; Xie, X.; Liu, M.; Yang, Q.; Wang, L.; et al. Robust soliton crystals in a thermally controlled microresonator. *Opt. Lett.* **2018**, *43*, 2002−2005.
(39) Geng, Y.; Huang, X.; Cui, W.; Ling, Y.; Xu, B.; Zhang, J.; Yi, X.; Wu, B.; Huang, S.-W.; Qiu, K.; Wong, C. W.; Zhou, H. Terabit optical OFDM superchannel transmission via coherent carriers of a hybrid chip-scale soliton frequency comb. *Opt. Lett.* **2018**, *43*, 2406−2409.
(40) Zhou, H.; Geng, Y.; Cui, W.; Huang, S.-W.; Zhou, Q.; Qiu, K.; Wei Wong, C. Soliton bursts and deterministic dissipative Kerr soliton generation in auxiliary-assisted microcavities. *Light: Sci. Appl.* **2019**, *8*, 50.
(41) Niu, R.; Wan, S.; Wang, Z.-Y.; Li, J.; Wang, W.-Q.; Zhang, W.-F.; Guo, G.-C.; Zou, C.-L.; Dong, C.-H. Perfect soliton crystals in the high-Q microrod resonator. *IEEE Photonics Technol. Lett.* **2021**, *33*, 788−791.
(42) Niu, R.; Li, M.; Wan, S.; Sun, Y. R.; Hu, S.-M.; Zou, C.-L.; Guo, G.-C.; Dong, C.-H. kHz-precision wavemeter based on reconfigurable microsoliton. *Nat. Commun.* **2023**, *14*, 169.
(43) Camatel, S.; Ferrero, V. Narrow linewidth CW laser phase noise characterization methods for coherent transmission system applications. *J. Lightwave Technol.* **2008**, *26*, 3048−3055.
(44) Kuse, N.; Fermann, M. Electro-optic comb based real time ultra-high sensitivity phase noise measurement system for high frequency microwaves. *Sci. Rep.* **2017**, *7*, 2847.
(45) Kuse, N.; Fermann, M. A photonic frequency discriminator based on a two wavelength delayed self-heterodyne interferometer for low phase noise tunable micro/mm wave synthesis. *Sci. Rep.* **2018**, *8*, 13719.
(46) Liu, J.; Lucas, E.; Raja, A. S.; He, J.; Riemensberger, J.; Wang, R. N.; Karpov, M.; Guo, H.; Bouchand, R.; Kippenberg, T. J. Photonic microwave generation in the X-and K-band using integrated soliton microcombs. *Nat. Photonics* **2020**, *14*, 486−491.
(47) Yao, L.; Liu, P.; Chen, H.-J.; Gong, Q.; Yang, Q.-F.; Xiao, Y.-F. Soliton microwave oscillators using oversized billion Q optical microresonators. *Optica* **2022**, *9*, 561−564.
(48) Yang, Q.-F.; Ji, Q.-X.; Wu, L.; Shen, B.; Wang, H.; Bao, C.; Yuan, Z.; Vahala, K. Dispersive-wave induced noise limits in miniature soliton microwave sources. *Nat. Commun.* **2021**, *12*, 1442.
(49) Weng, W.; Lucas, E.; Lihachev, G.; Lobanov, V. E.; Guo, H.; Gorodetsky, M. L.; Kippenberg, T. J. Spectral purification of microwave signals with disciplined dissipative Kerr solitons. *Phys. Rev. Lett.* **2019**, *122*, 013902.
(50) Liang, W.; Eliyahu, D.; Ilchenko, V. S.; Savchenkov, A. A.; Matsko, A. B.; Seidel, D.; Maleki, L. High spectral purity Kerr frequency comb radio frequency photonic oscillator. *Nat. Commun.* **2015**, *6*, 7957.
(51) Stone, J. R.; Briles, T. C.; Drake, T. E.; Spencer, D. T.; Carlson, D. R.; Diddams, S. A.; Papp, S. B. Thermal and nonlinear dissipative-soliton dynamics in Kerr-microresonator frequency combs. *Phys. Rev. Lett.* **2018**, *121*, 063902.
(52) Stern, B.; Ji, X.; Okawachi, Y.; Gaeta, A. L.; Lipson, M. Battery-operated integrated frequency comb generator. *Nature* **2018**, *562*, 401−405.
(53) Liu, Y.; Qiu, Z.; Ji, X.; Bancora, A.; Lihachev, G.; Riemensberger, J.; Wang, R. N.; Voloshin, A.; Kippenberg, T. J. A fully hybrid integrated Erbium-based laser. *arXiv* **2023**, arXiv:2305.03652.
(54) Kelleher, M. L.; McLemore, C. A.; Lee, D.; Davila-Rodriguez, J.; Diddams, S. A.; Quinlan, F. Compact, portable, thermal-noise-limited optical cavity with low acceleration sensitivity. *Opt. Express* **2023**, *31*, 11954−11965.




https://doi.org/10.1021/acsphotonics.3c01247
*ACS Photonics* 2024, 11, 1412−1418